30

The Ocean
Supplementary Material

Coordinating Lead Authors:
Ove Hoegh-Guldberg (Australia), Rongshuo Cai (China)

Lead Authors:
Elvira S. Poloczanska (Australia), Peter G. Brewer (USA), Svein Sundby (Norway), Karim Hilmi (Morocco), Victoria J. Fabry (USA), Sukgeun Jung (Republic of Korea)

Contributing Authors:
William Skirving (USA), Dáithí Stone (Canada/South Africa/USA), Michael T. Burrows (UK), Johann Bell (New Caledonia), Long Cao (China), Simon Donner (Canada), C. Mark Eakin (USA), Arne Eide (Norway), Benjamin Halpern (USA), Charles R. McClain (USA), Mary I. O'Connor (Canada), Camille Parmesan (USA), R. Ian Perry (Canada), Anthony J. Richardson (Australia), Christopher J. Brown (Australia), David Schoeman (Australia), Sergio Signorini (USA), William Sydeman (USA), Rui Zhang (China), Ruben van Hooidonk (USA), Stewart M. McKinnell (PICES/Canada)

Review Editors:
Carol Turley (UK), Ly Omar (Senegal)

Volunteer Chapter Scientists:
Jo Davy (New Zealand), Sarah Lee (USA)

Additional Information on Past, Present, and Future Ocean Conditions

These supplementary materials include further information on primary productivity and fisheries as well as past, present, and future (over the next 100 years) pH, Aragonite Saturation State, and Sea Surface temperatures (SST).

SM30.1. Primary Productivity and Long-Term Fisheries Catch

Different ocean sub-regions have substantially different primary and fishery productivities. Notably, over 80% of fisheries production is associated with three Ocean sub-regions: Northern hemisphere High Latitude Spring Bloom Systems (HLSBS-North), Coastal Boundary Systems (CBS), and Eastern Boundary Upwelling Ecosystems (EBUE; Table SM30-1, Figure 30-1b).

SM30.2. Definition as well as Coolest and Warmest Months for Key Ocean Sub-Regions Examined in Chapter 30

The HadISST1.1 data set (Rayner et al., 2003) was used to explore SST trends over the past 60 years (1950–2009; main text, Table 30-1), particularly in terms of long-term trends in average temperature as well as long-term trends in the coolest and warmest months of the year (Table SM30-2). The regions are outlined in Figure SM30-1 and Table SM30-2 (column 1). These data are discussed in the main text of Chapter 30 (Table 30-1).

Table SM30-1 | Percentage surface area of the ocean, average primary production, and fisheries productivity of key ocean sub-regions (Figure 30-1). Also shown are the primary IPCC assessments (by chapter number and sections of Chapter 30) that are relevant to each of the sub-regions. Details of calculations are as follows: (1) Calculation of the surface areas of the ocean sub-regions was made by transferring the boundary lines of the sub-regions to Google Maps and then using a graphical planimeter freeware provided in Google Maps. The planimeter program was made by Europa Technologies, MapLink, Tele Atlas, INEGI. (2) Calculation of primary production for each sub-region was carried out using a similar approach by transferring the original map of world primary production in Field et al. (1998) to the planimeter tool (freeware provided in Google Maps). Areas were weighted for each color scale value (g C m^{-2}) to get numbers in g C. These were summed for each area within a sub-region to get total values of g C. (3) Calculation of fish catch for each sub-region was based on the FAO Statistics on world fish catch in their standard regional areas (1–88). However, as the FAO standard catch areas do not completely resolve the spatial areas of the sub-regions and partly cross different ocean sub-regions of Chapter 30, the division of fish catches in Large Marine Ecosystems (LMEs, as displayed in the project The Sea Around Us: http://www.seaaroundus.org/) was used to correct the numbers. The data from this source are, however, also based on the same FAO Fish Statistics. *Based on Field et al. (1998); **Average fish catch 1970–2006 Based on FAO; ***Not calculated.

Ocean sub-region		Area (%)	Primary productivity (%)*	Long-term fish catch (%)**	Relevant IPCC regions (chapters)	Chapter 30 sections
1. High Latitude Spring Bloom System (HLSBS)	Northern Hemisphere	10.60	22.74	29.20	23–24, 26, 28	30.5.6, 30.6.2.1, Box CC-MB
	Southern Hemisphere	14.40	20.55	6.82	22, 25, 28	30.5.6
2. Equatorial Upwelling Systems (EUS)		8.20	9.01	4.68	22, 27, 29	30.5.3, 30.6.2.1, Box CC-CR
3. Semi-Enclosed Seas (SES)		1.12	2.35	3.28	22, 23	30.5.5
4. Coastal Boundary Systems (CBS)		6.29	10.64	28.02	22, 24–26, 29	30.5.4, 30.6.2.1, Box CC-CR
5. Eastern Boundary Upwelling Systems (EBUE)		1.80	6.97	19.21	22, 26, 27	30.5.5, Box CC-UP
6. Sub-Tropical Gyres (STG)		40.55	21.20	8.26	22, 24–26, 29	30.5.6, 30.6.2.1, Box CC-PP, Box CC-CR
7. Deep Sea (DS)***		N/A	N/A	N/A	22–29	30.5.7
Arctic and Antarctic System		17.04	6.54	0.53	23, 24, 25, 26	

Table SM30-2 | The coolest and warmest months for ocean sub-regions identified in Figure SM30-1. Entire regions (e.g., Indian Ocean) or parts of sub-regions (e.g., eastern portion of the North Pacific Ocean) are indicated by letters in the first column that relate to those inscribed on Figure SM30-1. Coolest and hottest months were identified from an analysis of the last 60 years of sea surface temperature using the HadISST1.1 dataset (Rayner et al., 2003).

| Sub-region	Map component (see Figure SM30-1)	Area	Coolest month	Warmest month
1. High Latitude Spring Bloom Systems (HLSBS)	A	Indian Ocean	September	February
	B	North Atlantic Ocean	March	August
	C	South Atlantic Ocean	August	February
	D	North Pacific Ocean (west)	March	August
	E	North Pacific Ocean (east)	March	August
	D+E	North Pacific Ocean	March	August
	F	South Pacific Ocean (west)	September	February
	G	South Pacific Ocean (east)	September	February
	F+G	South Pacific Ocean	September	February
2. Equatorial Upwelling Systems (EUS)	H	Atlantic Equatorial Upwelling	August	April
	I	Pacific Equatorial Upwelling	September	April
3. Semi-Enclosed Seas (SES)	J	Arabian Gulf	February	August
	K	Baltic Sea	March	August
	L	Black Sea	March	August
	M	Mediterranean Sea	February	August
	N	Red Sea	February	August
4. Coastal Boundary Systems (CBS)	O	Western Atlantic	August	March
	P	Caribbean Sea/Gulf of Mexico	February	September
	Q	Indian Ocean (west)	August	May
	R	Indian Ocean (east)	August	April
	S	Indian Ocean (east)/Southeast Asia/Pacific Ocean (west)	February	August
5. Eastern Boundary Upwelling Ecosystems (EBUE)	T	Benguela Current	August	March
	U	California Current	March	September
	V	Canary Current	February	September
	W	Humboldt Current	September	February
6. Sub-Tropical Gyres (STG)	X	Indian Ocean	August	March
	Y	North Atlantic Ocean	March	August
	Z	South Atlantic Ocean	September	March
	AA	North Pacific Ocean (west)	February	August
	AB	North Pacific Ocean (east)	February	September
	AA+AB	North Pacific Ocean	February	September
	AC	South Pacific Ocean (west)	August	February
	AD	South Pacific Ocean (east)	September	February
	AC+AD	South Pacific Ocean	September	February
Coral Reef Provinces	See Figure 30-4(b)	Caribbean Sea/Gulf of Mexico	February	September
		Coral Triangle and Southeast Asia	February	May
		Indian Ocean (east)	August	April
		Indian Ocean (west)	August	April
		Pacific Ocean (east)	December	August
		Pacific Ocean (west)	August	February
Basin Scale	B+Y	North Atlantic Ocean	March	August
	C+Z	South Atlantic Ocean	September	March
	B+Y+H+Z+C	Atlantic Ocean	December	August
	E+AB+D+AA	North Pacific Ocean	March	August
	AD+G+AC+F	South Pacific Ocean	August	February
	E+AB+I+AD+G+D+AA+AC+F	Pacific Ocean	December	August
	Q+X+A	Indian Ocean	August	April
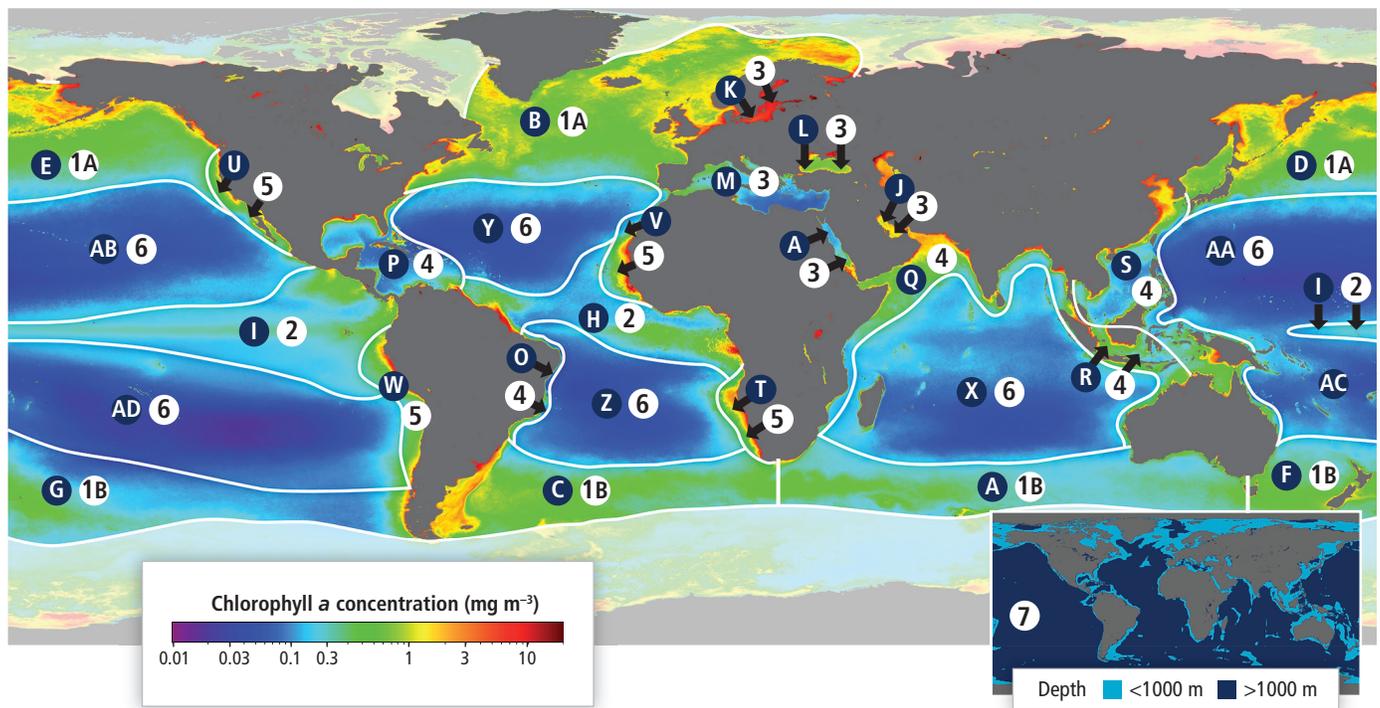
Figure SM30-1 | The seven major sub-regions of the Ocean used in Chapter 30 (numbered) and areas identified in Table SM30-2 (marked with letters). The chlorophyll-*a* concentration averaged over the period from SeaWiFS (Sep 1997–30 Nov 2010; NASA) is provides a proxy for differences in marine productivity (with the caveats provided in Box CC-PP). Key oceanographic features and primary production was the basis for separating the ocean into the sub-regions shown (Section 30.1.1, Table SM30-1). The map insert shows the distribution of Deep Sea habitat (1000 m; Bathypelagic and Abyssopelagic habitats combined).

SM30.3. Sea Surface Temperatures under RCP2.6, RCP4.5, RCP6.0, and RCP8.5

Projections of future SST changes were examined for sub-regions and areas within sub-regions (Figure SM30-1) using ensemble averages from AOGCM simulations available in the CMIP5 archive (Table SM30-3) for the four representative concentration pathways (RCP2.6, RCP4.5, RCP6.0, and RCP8.5; van Vuuren et al., 2011). Ensemble averages for each RCP are based on simulations from 10 to 16 individual models (Table SM30-3). Model hind-casts matched those observed for ocean sub-regions for the period 1980–2009 (HadISST1.1; Table SM30-2, Figure SM30-1), but with the AOGCM ensemble slightly overestimating the extent of change across the different ocean sub-regions (slope of observed/model = 0.81, r^2 = 0.76, p<0.001). In this way, the absolute change projected to occur in the ocean sub-regions was calculated for near-term (over 2010–2039) and long-term (over 2070–2099) periods (Table SM30-4). In the near term, projected changes in SST are largely indistinguishable between the different RCP pathways due to similarity in forcing until 2030s. Over the long-term, however, SSTs across the Ocean sub-regions were 1–3°C higher under RCP8.5 than those projected to occur under RCP2.6 (Table SM30-4). The implications of these projected changes on the structure and function of oceanic systems are extensively discussed in Chapters 6 and 30.

Table SM30-3 | CMIP5 model simulations used to create the Representative Concentration Pathway (RCP) 2.6, 4.5, 6.0, and 8.5 SST ensembles used in Chapter 30. The subset of CMIP5 models was chosen because each has historic runs enabling the derivation of the Maximum Monthly Mean (MMM) climatology over 1985 to 2000, ensuring that all anomalies were comparable across time periods and across RCPs. All models indicated were used to ensemble SSTs as well as to produce Degree Heating Month (DHM) measurements, with the exception of 2 model outputs, denoted by a * (which could not generate reliable MMM climatologies).

CMIP5 Model	RCP2.6	RCP4.5	RCP6.0	RCP8.5
ACCESS1-0		1		1
ACCESS1-3		1		1
BCC-CSM1-1	1	1	1	1
CanESM2	1	1		1
CMCC-CM		1		1
CMCC-CMS		1		1
CNRM-CM5	1	1		1
CSIRO-Mk3-6-0	1	1	1	1
EC-EARTH	*	1		1
FIO-ESM	1	1	1	1
GFDL-CM3	1	1	1	1
GFDL-ESM2G	1	1	1	1
GFDL-ESM2M	1	1		1
GISS-E2-R-p1	1	1	1	1
GISS-E2-R-p2	1	1	1	1
GISS-E2-R-p3	1	1	1	1
HadGEM2-AO	1	1	1	1
HadGEM2-CC		1		1
HadGEM2-ES	1	1	1	1
INMCM4		1		1
IPSL-CM5A-LR	1	1	*	1
IPSL-CM5A-MR	1	1		1
MPI-ESM-LR	1	1		1
MPI-ESM-MR	1	1		1
CESM1-BGC		1		1
CESM1-CAM5	1	1	1	1
NorESM1-M	1	1	1	1
NorESM1-ME	1	1	1	1
Number of models	20+1*	28	13+1*	28

Table SM30-4 | Projected changes in sea surface temperature (SST ˚C) over the next 90 years for ocean sub-regions (Figure SM30-1) from AOGCM model simulations from the Coupled Model Intercomparison Project Phase 5 (CMIP5, http://cmip-pcmdi.llnl.gov/cmip5/). Simulations were available for four Representative Concentration Pathways (RCPs): RCP2.6, RCP4.5, RCP6.0, and RCP8.5. The CMIP5 models used in this analysis are listed in Table SM30-3. For each ocean sub-region, a linear regression was fitted to all 1x1 degree monthly SST data extracted from the models for each of three periods; 2010–2039, 2040–2069, and 2070–2099. The average change in SST was calculated by multiplying the slope of each linear regression by 360 (months) to derive the average change over each successive 30-year period. The table is divided into two sections: "Near-term (2010–2039)" (the average change in SST over the next 30 years) and "Long-term (2010–2099)" (the total change over 2010–2099, which was calculated by adding the average change of the three 30-year periods from 2010 to 2099). This is a simplified method to account for slight non-linearity in SST change over the 90-year period.

Sub-region	Area	Near-term (2010–2039)				Long-term (2010–2099)				RCP8.5 minus RCP2.6
		RCP2.6	RCP4.5	RCP6.0	RCP8.5	RCP2.6	RCP4.5	RCP6.0	RCP8.5	
1. High Latitude Spring Bloom Systems (HLSBS)	Indian Ocean	0.13	0.29	0.18	0.41	−0.16	0.49	0.83	2.01	2.17
	North Atlantic Ocean	0.31	0.56	0.52	0.65	0.54	1.54	1.95	3.02	2.48
	South Atlantic Ocean	0.17	0.36	0.20	0.45	−0.09	0.67	0.88	2.26	2.36
	North Pacific Ocean (west)	0.79	0.96	0.91	1.17	1.46	2.47	3.07	4.84	3.38
	North Pacific Ocean (east)	0.79	0.81	0.93	1.06	1.31	2.17	2.96	4.39	3.08
	North Pacific Ocean	0.79	0.88	0.92	1.11	1.35	2.31	3.01	4.60	3.25
	South Pacific Ocean (west)	0.17	0.40	0.25	0.50	−0.16	0.63	0.85	2.37	2.53
	South Pacific Ocean (east)	0.12	0.23	0.13	0.35	−0.09	0.45	0.75	1.70	1.79
	South Pacific Ocean	0.14	0.28	0.17	0.40	−0.12	0.51	0.78	1.91	2.03
2. Equatorial Upwelling Systems (EUS)	Atlantic Equatorial Upwelling	0.43	0.58	0.49	0.81	0.46	1.19	1.61	3.03	2.56
	Pacific Equatorial Upwelling	0.35	0.55	0.54	0.77	0.43	1.22	1.75	3.01	2.57
3. Semi-Enclosed Seas (SES)	Arabian Gulf	0.82	0.97	0.89	1.20	1.30	2.39	2.96	4.26	2.96
	Baltic Sea	0.73	1.24	0.92	1.20	1.32	2.74	3.06	4.37	3.05
	Black Sea	0.74	1.01	0.86	1.24	1.37	2.61	3.16	4.19	2.82
	Mediterranean Sea	0.72	0.87	0.84	1.09	1.37	2.10	2.82	4.08	2.70
	Red Sea	0.56	0.72	0.71	0.93	0.88	1.65	2.39	3.45	2.57
4. Coastal Boundary Systems (CBS)	Atlantic Ocean (west)	0.34	0.40	0.45	0.62	0.23	0.81	1.33	2.44	2.21
	Caribbean Sea/Gulf of Mexico	0.50	0.67	0.64	0.85	0.74	1.53	1.97	3.23	2.49
	Indian Ocean (west)	0.46	0.59	0.56	0.85	0.63	1.39	1.95	3.32	2.69
	Indian Ocean (east)	0.34	0.57	0.46	0.69	0.38	1.22	1.59	2.80	2.42
	Indian Ocean (east), Southeast Asia, Pacific Ocean (west)	0.48	0.66	0.57	0.82	0.66	1.47	1.89	3.12	2.46
5. Eastern Boundary Upwelling Ecosystems (EBUE)	Benguela Current	0.30	0.43	0.45	0.71	0.07	0.70	1.41	2.52	2.45
	California Current	0.62	0.71	0.84	0.93	1.02	1.86	2.46	3.51	2.49
	Canary Current	0.55	0.62	0.58	0.82	0.97	1.30	1.83	3.18	2.21
	Humboldt Current	0.22	0.43	0.34	0.60	0.11	0.91	1.22	2.58	2.47
6. Sub-Tropical Gyres (STG)	Indian Ocean	0.30	0.44	0.37	0.63	0.19	0.89	1.35	2.62	2.43
	North Atlantic Ocean	0.49	0.66	0.60	0.85	0.87	1.62	1.98	3.30	2.43
	South Atlantic Ocean	0.25	0.33	0.33	0.55	0.03	0.58	1.03	2.20	2.18
	North Pacific Ocean (west)	0.54	0.70	0.64	0.90	0.84	1.62	2.08	3.39	2.55
	North Pacific Ocean (east)	0.56	0.66	0.71	0.91	0.90	1.56	1.50	3.44	2.54
	North Pacific Ocean	0.55	0.68	0.68	0.90	0.87	1.58	2.09	3.42	2.55
	South Pacific Ocean (west)	0.31	0.44	0.34	0.62	0.12	0.88	1.19	2.56	2.44
	South Pacific Ocean (east)	0.17	0.27	0.21	0.45	−0.03	0.52	0.89	1.90	1.93
	South Pacific Ocean	0.20	0.31	0.24	0.49	0.00	0.60	0.96	2.05	2.05
Coral Reef Provinces; see Figure 30-4b	Caribbean Sea/Gulf of Mexico	0.48	0.64	0.61	0.83	0.68	1.43	1.87	3.14	2.46
	Coral Triangle and Southeast Asia	0.42	0.61	0.52	0.76	0.58	1.35	1.75	2.95	2.37
	Indian Ocean (east)	0.32	0.56	0.46	0.67	0.37	1.18	1.59	2.76	2.40
	Indian Ocean (west)	0.39	0.51	0.50	0.77	0.43	1.18	1.71	2.97	2.54
	Pacific Ocean (east)	0.46	0.64	0.64	0.83	0.63	1.44	1.99	3.23	2.60
	Pacific Ocean (west)	0.35	0.48	0.40	0.68	0.30	1.02	1.39	2.66	2.35

Table SM30-4 (continued)

Sub-region	Area	Near-term (2010–2039)				Long-term (2010–2099)				RCP8.5 minus RCP2.6
		RCP2.6	**RCP4.5**	**RCP6.0**	**RCP8.5**	**RCP2.6**	**RCP4.5**	**RCP6.0**	**RCP8.5**	
Basin Scale	North Atlantic Ocean	0.37	0.60	0.55	0.72	0.66	1.57	1.96	3.12	2.46
	South Atlantic Ocean	0.21	0.35	0.27	0.51	−0.03	0.62	0.76	2.23	2.26
	Atlantic Ocean	0.32	0.50	0.44	0.65	0.38	1.17	1.54	2.78	2.40
	North Pacific Ocean	0.64	0.75	0.77	0.98	1.06	1.85	2.43	3.86	2.80
	South Pacific Ocean	0.18	0.30	0.21	0.45	−0.04	0.56	0.89	2.00	2.04
	Pacific Ocean	0.41	0.54	0.51	0.73	0.52	1.23	1.70	2.97	2.45
	Indian Ocean	0.30	0.44	0.37	0.63	0.19	0.89	1.35	2.62	2.43

30

SM30.4. Changes to Surface pH and Aragonite Saturation State under Different Concentrations of Atmospheric CO_2

The relative changes in pH and the aragonite saturation state of seawater varies in concert with increases in the partial pressure of CO_2 above the ocean. Observations of ocean chemistry (Doney et al., 2009; Feely et al., 2009) are highly consistent with models of the carbonate chemistry of the upper ocean (Caldeira and Wickett, 2003). Notably, high latitude areas, as well as regions where upwelling is dominant, show naturally lower pH and aragonite saturation states. These regions are expected to reach critical levels in terms of pH and aragonite saturation sooner than lower latitudes and non-upwelling regions (Section 30.3.2.2).

(a) Ocean pH as a function of atmospheric CO_2 concentration
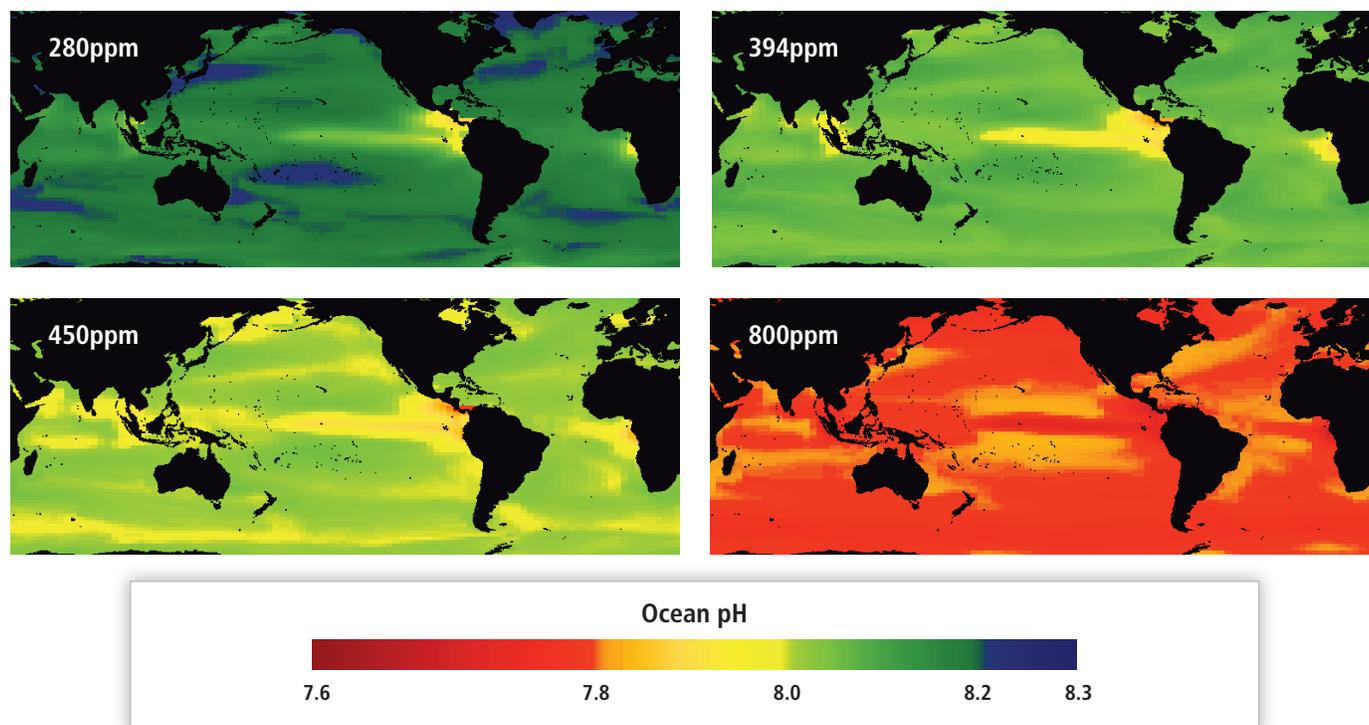
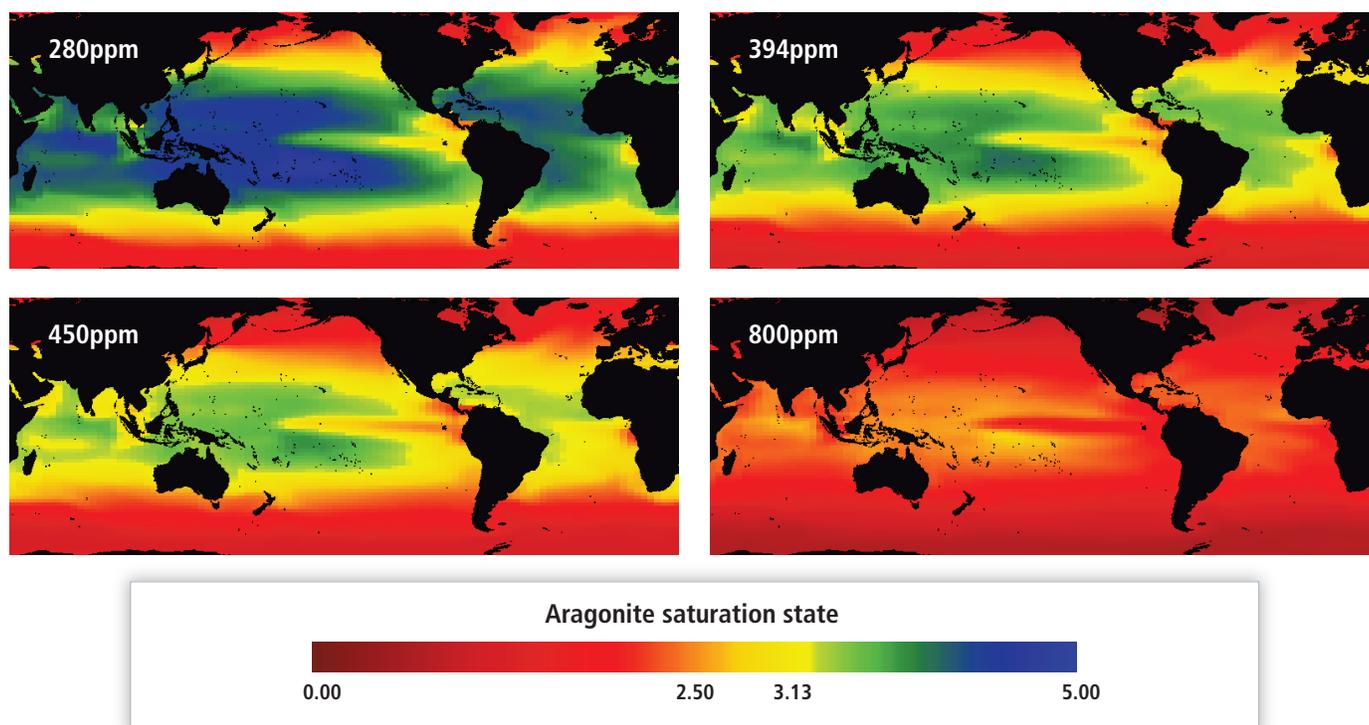## (b) Aragonite saturation state

Figure SM30-2 | The carbonate chemistry of the Ocean under current different atmospheric concentration s of CO_2. 280ppm represents pre-industrial and 394ppm present-day levels (WGI Annex II). (a) Surface pH and (b) Aragonite saturation state of the Ocean simulated by the University of Victoria Earth System Model. The fields of pH and aragonite saturation state are calculated from the model output of dissolved inorganic carbon concentration, alkalinity concentration, temperature, and salinity, together with the chemistry routine from the OCMIP-3 project (http://www.ipsl.jussieu.fr/OCMIP/phase3).

SM30.5. Projections of Changes to Sea Surface Temperatures (RCP2.6 and RCP8.5) for Different Regions that have Coral Reefs

Warm-water coral reefs throughout the world (but particularly in CBS, SES, and STG; Figure SM30-1) are rapidly declining as result of local perturbations (i.e., coastal pollution, overexploitation) and climate change (*high confidence*; Sections 30.5.3-4, 30.5.6). Reef-building corals, which are responsible for building the carbonate framework of coral reefs, are sensitive to both elevated sea temperatures as well as reduced pH and carbonate concentrations (*high confidence*; Section 6.3.2; Boxes CC-CR, CC-OA). Continued increases in sea temperature will increase the incidence of impacts such as mass coral bleaching and mortality (*virtually certain*), with the CMIP5 ensemble projecting the irreversible degradation of coral reefs from most sites globally by 2050 (*very likely*; Section 30.5; Figure 30-10; Box CC-CR). Investigating past, present, and future sea temperatures in six major coral reef areas (Figure 30-4b) reveals that future sea temperatures will exceed established thresholds of coral bleaching and mortality around the middle to late part of this century (Figure SM30-3).

References

Caldeira, K. and M. E. Wickett, 2003: Oceanography: anthropogenic carbon and ocean pH. *Nature*, **425(6956)**, 365-365.

Doney, S.C., V.J. Fabry, R.A. Feely, and J.A. Kleypas, 2009: Ocean acidification: the other CO_2 problem. *Annual Review of Marine Science*, **1**, 169-192.

Feely, R.A., S.C. Doney, and S.R. Cooley, 2009: Ocean acidification: present conditions and future changes in a high-CO_2 world. *Oceanography*, **22(4)**, 36-47.

Field, C.B., M.J. Behrenfeld, J.T. Randerson, and P. Falkowski, 1998: Primary production of the biosphere: integrating terrestrial and oceanic components. *Science*, **281**, 237-240.

Rayner, N.A., D.E. Parker, E.B. Horton, C.K. Folland, L.V. Alexander, D.P. Rowell, E.C. Kent, and A. Kaplan, 2003: Global analyses of sea surface temperature, sea ice, and night marine air temperature since the late nineteenth century. *Journal of Geophysical Research*, **108(D14)**, 4407.

van Vuuren, D.P., J. Edmonds, M. Kainuma, K. Riahi, A. Thomson, K. Hibbard, G.C. Hurtt, T. Kram, V. Krey, J.-F. Lamarque, T. Masui, M. Meinshausen, N. Nakicenovic, S.J. Smith, and S.K. Rose, 2011: The representative concentration pathways: an overview. *Climatic Change*, **109**, 5-31.
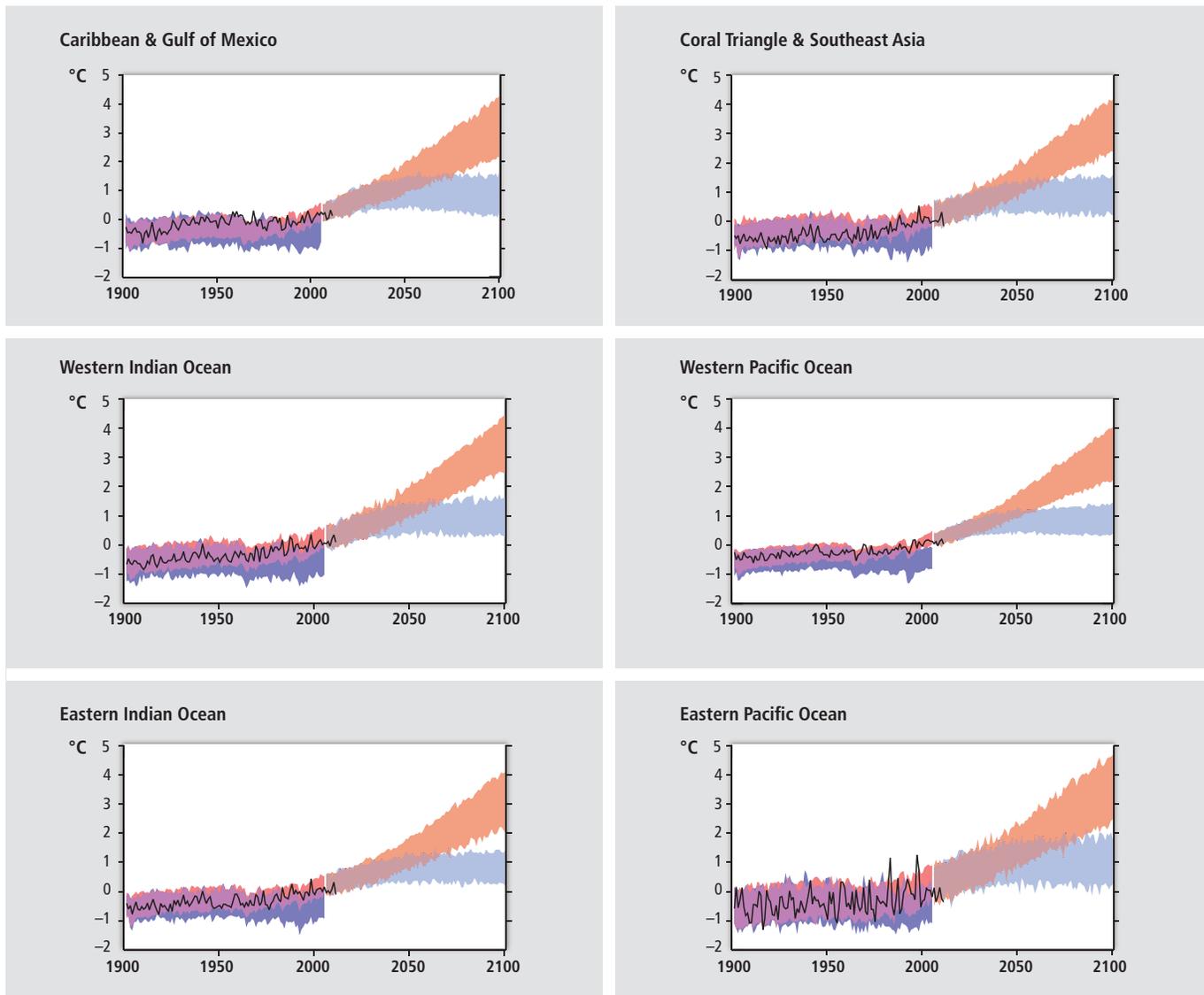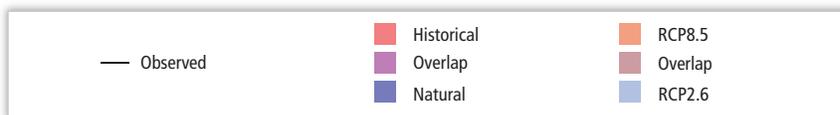
30

Figure SM30-3 | Past and future sea surface temperatures (SST) in six major coral reef provinces and locations (Figure 30-4b) under historic, un-forced (natural), RCP2.6 and RCP8.5 scenarios from CMIP5 ensembles (Table SM30-3). Observed and simulated variations in past and projected future annual average SST over various sites where coral reefs are prominent ecosystems (locations shown in Figure 30-4b). The black line shows estimates from HadISST1.1 [Rayner et al., 2003] reconstructed historical SST dataset. Shading denotes the 5–95 percentile range of climate model simulations driven with 'historical' changes in anthropogenic and natural drivers (62 simulations), historical changes in 'natural' drivers only (25), the RCP4.5 emissions scenario (62), and the RCP8.5 (62). Data are anomalies from the 1986–2006 average of the HadISST1.1 data (for the HadISST1.q time series) or of the corresponding historical all- forcing simulations. Further details are given in Box 21.1, 21.3.